CHAPTER III

OBSERVATIONS AND DATA REDUCTION

This chapter presents general information on the radio-astronomical observations, instruments, data reduction and data analysis studied in this thesis. The data reduction techniques for spectral line polarization observations are described in detail.

3.1 Radio Observations

Most of the radio observations described in this thesis have been made using the Multi-Element-Radio-Link-Interferometer-Network (MERLIN). It consists of a number of individual antennae, or telescopes, which are effectively connected in pairs to form a collection of two-element interferometers or a synthesis array.

The output from an interferometer is formed by multiplying together the complex voltages received by the two antennae and integrating. The voltages must be considered to be complex since the paths along which the signals travel before being multiplied together are not the same, and so they have both a magnitude (or amplitude) and a phase term.

Consider the simple interferometer shown in Figure 3.1 in which the two antennae, physically separated by a distance, L = N $\times\lambda$, where λ is the wavelength of the radio waves, are pointing at a region of sky in a direction, θ. It can be shown that the output voltage from the multiplier is

$$V_{out} = V_1 V_2 \; exp\; (-i\phi)$$

where the phase term,

$$\phi = (2\pi N cos\; \theta - \tau)$$

represents the path difference between the two signals input to the mutiplier. If the path difference, τ, is constantly adjusted so that

$$(2\pi N cos\; \theta - \tau) = 0,$$

then the output voltage

$$V_{out} = V_1 V_2$$

which is a constant.

However, consider the signal arriving at the antennae from a slightly different direction $(\theta + \alpha)$. The output from the interferometer is:-

$$V_{out} = V_1 V_2 \; exp{-}i(2\pi N cos(\theta + \alpha) - \tau)$$

For small angles, α, where sin $\alpha \approx \alpha$ and cos $\alpha \approx 1$, and putting (2π N cos θ - τ) = 0 as above, then the output becomes:-

$$V_{out} = V_1 V_2 \; exp\; 2\pi i\; (N\; sin\; \theta).\; \alpha) - \tau) = V_1 V_2 \; exp\; 2\pi i\; u'\; \alpha$$

since u', which is the projected separation of the two telescopes in wavelengths, is N sin θ. This projected separation or spacing, u', which is in a two-dmensional plane on the sky for small angles, can be resolved into 'u' and 'v' components, in which the axes, u,v, are chosen such that the angle, α, is resolved into real angles on the sky in directions corresponding to right ascension and declination. This imaginary plane in the sky is referred to as the uv-plane. Thus the interferometer output becomes

$$V_{out} = V_1 V_2 \; exp \; 2\pi i \; (u \; \alpha' + v \; \delta')$$

where α' and δ' are real angles on the sky relative to the direction, θ, in which the antennae are pointing.

In reality, the voltages V_1 and V_2 are a summation of all the signals in the sky entering the antennae, and so the output from the interferometer at any instant of time can be written

$$v_{out} = C \int \int T_s(\alpha', \delta') \sqrt{A_1(\alpha', \delta') \; A_2(\alpha', \delta') \; exp(2\pi i(u \; \alpha' + v \; \delta'))} \; d\alpha' d\delta')$$

where the $T_s \; (\alpha', \delta')$ represent the sky signals converted to equivalent temperatures and $A_i \; (\alpha', \delta')$ represent the gains of the antennae. Thus, the output from an interferometer at any instant of time is a Fourier component of the sky brightness distribution, and an image or map of the observed radio source can be made by inverse Fourier transform of the 'visibilities' data, which is what the output from an interferometer is often called. Unfortunately, the amplitude and phase of the visibilities are changed by many factors, such as by the characteristics of the instrument itself, equipment variations during the observation time, the elevation of the antennae, and especially by the Earth's atmosphere. Thus, before Fourier transforming the visibilities data to produce images, the data must be calibrated to remove these unwanted effects. The calibration that needs to be carried out by the observer is defined as the third level calibration by Perley et al. (1989). Standard calibration sources, which must be observed in each observing session, are a phase calibrator for measurement of changes in the paths of the signals through the atmosphere, flux calibrators, which measure the antennae sensitivities, and a polarization calibrator. The phase calibrator must be chosen from a list of calibration sources which are close to the target source to be observed so that the signals from both the target and phase-reference sources travel through almost the same paths through the atmosphere. Data editing before and after calibration are usually necessary because of equipment malfunction and often large atmospheric changes during the integration time for each data point measurement.

3.2 MERLIN

The Multi-Element-Radio-Linked-Interferometer-Network (MERLIN)[1] is an array of seven antennae: Cambridge, Defford, Knockin, Darnhall, Mark 2, Lovell and Tabley. All of the antennae are permanently linked to Jodrell Bank, from

[1]MERLIN is a National Facility operated by the University of Manchester on behalf of the Science Technology Facilities Council.

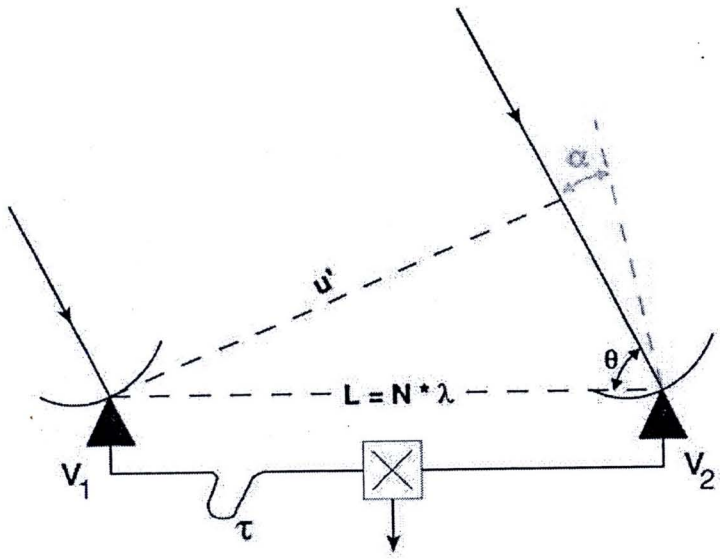

Figure 3.1 A Simple two-element interferometer.

where they can be controlled remotely. Figure 3.2 shows the location of each of the MERLIN antennas and the paths between the microwave links at each outstation and Jodrell Bank.

As already indicated, each pair of antennas forms an interferometer which, at any instant of time, measures a component of the two-dimensional Fourier transform (the visibility function) of the sky brightness distribution within the primary beam of an individual antenna. The projection of the baseline onto the plane of the incident wavefront can be resolved into two components (u, v), where u is towards the East and v is toward the North. During observations, the rotation on of the Earth continually changes the orientation of each baseline, such that the Fourier component measured changes with time. In fact each projected baseline sweeps out an ellipse in the (u, v) plane. The source brightness distribution can then be recovered by inverse Fourier transformation of the visibility data.

MERLIN can operate in any one of five different observing bands: UHF-band (151 MHz), P-band (408 MHz), L-band (1.4 and 1.6 GHz), C-band (5 and 6 - 7 GHz) and K-band (22 GHz). The MERLIN data obtained for this thesis were observed at L- band covering the 4 OH maser spectral lines at 1612, 1665, 1667 and 1720 MHz, and C-band covering 2 OH maser spectral lines at 6035 and 6031 MHz and also the methanol maser at 6668 MHz. K-Band observations have also been made at the water line frequency at 22 GHz. The operation of MERLIN and detailed data reduction procedures can be found in the MERLIN *UserGuide* (2003) and the AIPS *Cookbook* (2003). The principles of interferometry are described in more detail in many textbooks (see for example: Thompson et al. 1986 Perley et al., 1989).

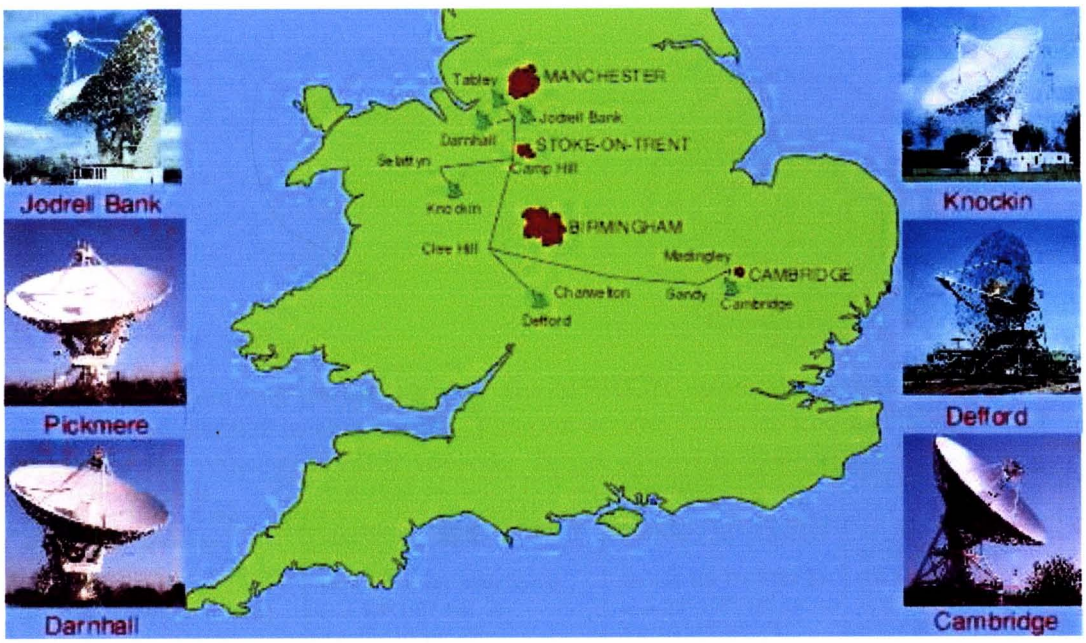

Figure 3.2 Location and photographs of the MERLIN telescopes.

3.3 The Observations

3.3.1 OH Maser at 1.6 GHz

All 4 ground state OH masers were observed in the star-forming regions, S140-IRS1 and W49A during the period 2005 May 5 - 10 and June 11-16, respectively using MERLIN (including the Lovell telescope). The longest baseline was 217km, giving a synthesised beam of ~ 0.15 arcsec. The total observing bandwidth of 256 kHz was divided into 512 channels resulting in a total velocity range of 45 km s^{-1} and a velocity resolution of ~ 0.09 km s^{-1}. The radial velocities relative to the local standard of rest (LSR) at the centre of the 250 kHz bands were –8 km s^{-1} for S140-IRS1 and +10 km s^{-1} for W49 A. Left- and right-hand circularly polarized signals from all pairs of telescopes were simultaneously correlated to give LL, LR, RL, RR polarized signals and hence all 4 Stokes parameters. The observations of both the main lines (1665 and 1667 MHz) and the satellite lines (1720 and 1612 MHz) took place over approximately 20 hours for each source, However, the time actually on a 'target' source was less than this as short scans on a nearby unresolved phase calibrator source were interleaved with the target source scans. Short ($\sim$ 30 min) scans were also made of amplitude and polarization position angle calibrator sources. Table 3.1 and 3.2 list the details of the observations and Figure 3.3 and 3.4 show examples of the u - v coverage at a wavelength of 18-cm for S140-IRS1 and W49 A respectively.

Table 3.1 Observing parameters for the MERLIN spectral-line polarization observations presented in this thesis. Time on source includes frequent short observations of the phase calibrator sources. Target source is S140-IRS1.

Target source name	S140-IRS1	S140-IRS1	S140-IRS1
Frequency Used (GHz)	1.6	6.0	22.2
Date of observations	May 5 - 10, 2005	February 14 - 15, 2008	24 Jan, 01 Feb 1998 & 23 Apr 2004
Antennas used[2]	De Ca Kn Da Mk2 Ta Lo	De Ca Kn Da Mk2 Ta	Ca Da Kn Mk2 Ta
Pointing positions (J2000)	$\alpha = 22^h19^m\ 18^s.22$ $\delta = 63°18'46''.78$	$\alpha = 22^h19^m\ 18^s.22$ $\delta = 63°18'46''.78$	$\alpha = 22^h19^m\ 18^s.22$ $\delta = 63°18'46''.78$
Central velocity (km s^{-1})	−8	−8	−5
Distance (pc)	764±27 (Hirota et al., 2008)	764±27	764±27
Central frequency (MHz)	1665.402 1667.359 1612.231 1720.530	6035.093	
Number of channels	512	512	256
Total bandwidth (MHz)	0.256	0.500	4000
Time on source	25h 33m	11h 41m	11h
Amplitude calibrator source for the target source	3C84	3C84	3C273
Number channels used	30-500	30-500	20-245
Phase calibrator source for the target source	2221+625	2221+625	2221+625
Central frequency (MHz)	1662.800 1612.400 1720.400	6034.800	
Number channels	16	16	
Total bandwidth (MHz)	16	16	
Amplitude calibrator source for the phase calibrator	3C84	3C84	3C273
Polarisation position angle calibrator source	3C286	3C286	
Number channel used	30-500	30-500	20-245

[2]Key for antenna abbreviations is shown in Table 3.3.

Table 3.2 Observing parameters for the MERLIN spectral-line polarization observations presented in this thesis. Time on source includes frequent short observations of the phase calibrator sources. Target source is W49 A.

Target source name	W49 A	W49 A	W49 A
Frequency used (GHz)	1.6	6.0	6.7
Date of observations	June 11 - 16, 2005	February 12 - 13, 2006	February 12 - 13, 2006
Antennas used	De Ca Kn Da Mk2 Ta	De Ca Kn Da Mk2 Ta	De Ca Kn Da Mk2 Ta
Pointing positions (J2000)	$\alpha = 19^h10^m\ 15^s.31$	$\alpha = 19^h10^m\ 15^s.31$	$\alpha = 19^h10^m\ 15^s.31$
	$\delta = 09°06'08''.48$	$\delta = 09°06'08''.48$	$\delta = 09°06'08''.48$
Central velocity (km s^{-1})	+10	+10	+10
Distance (kpc)	11.4±1.2 (Gwinn et al., 1992)	11.4±1.2	11.4±1.2
Central frequency (MHz)	1665.402	6030.749	6668.518
	1667.359	6035.093	
	1612.231		
	1720.530		
Number of channels	512	512	512
Total bandwidth (MHz)	0.256	0.256	0.256
Time on source	20h 58m	7h 50m	4h 5m
Amplitude calibrator source for the target source	3C84	3C84	3C84
Number channels used	30-500	30-500	30-500
Phase calibrator source for the target source	1919+086	1919+086	1919+086
Central frequency (MHz)	1662.800	6034.800	6670.000
	1612.400		
	1720.400		
Number channels	16	16	16
Total bandwidth (MHz)	16	16	16
Amplitude calibrator source for the phase calibrator	3C84	3C84	3C84
Polarization position angle calibrator source	3C286	3C286	3C286
Number channel used	30-500	30-500	30-500

Table 3.3 Key to antenna abbreviations

Telescope	Defford	Cambridge	Darnhall	Knockin	Mark 2	Pickmere	Lovell
Abbreviation	De	Ca	Da	Kn	Mk2	Pi	Lo
Weighting Factor	0.61	1.74	0.73	0.61	1.00	0.77	30.25

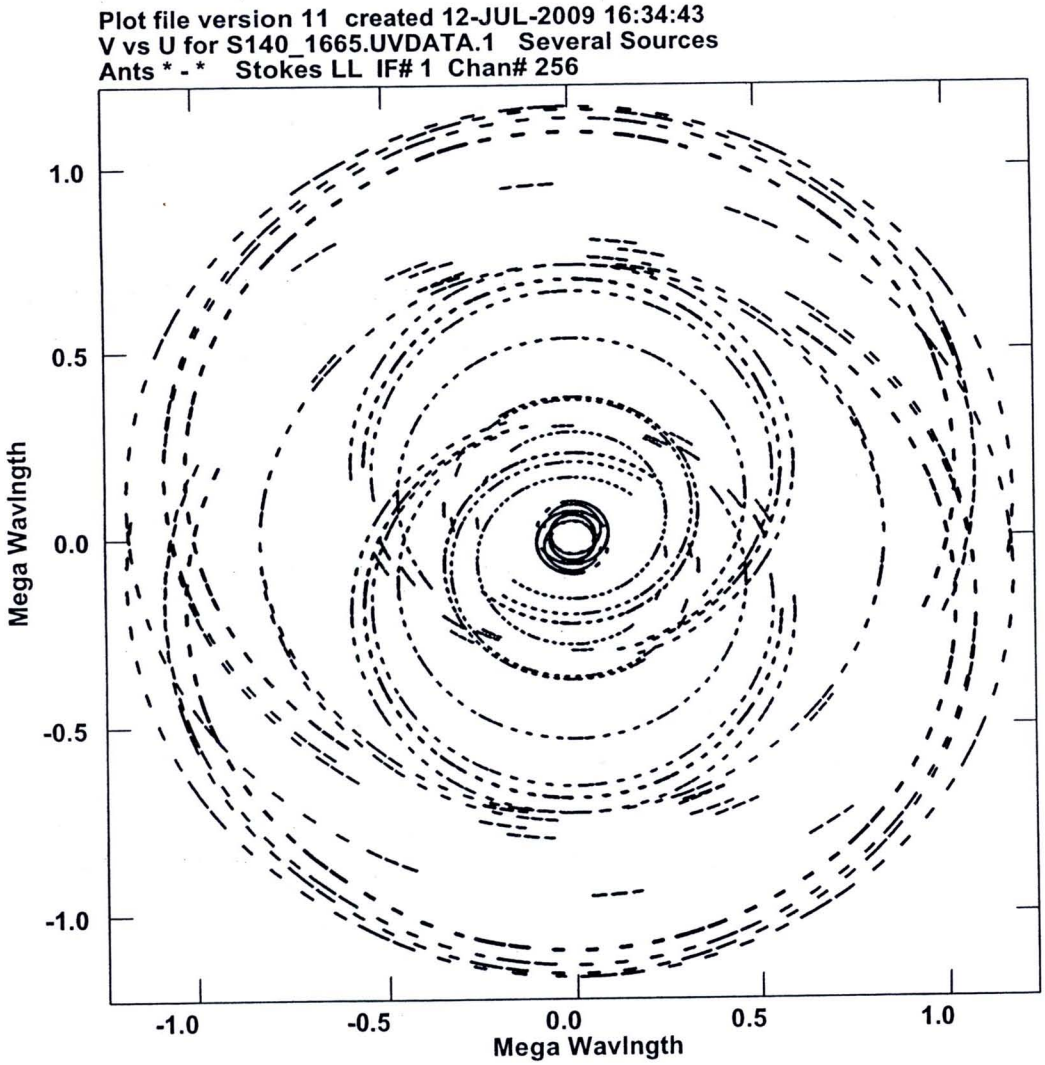

Figure 3.3 The u - v coverage at 1665 MHz for the source S140-IRS1.

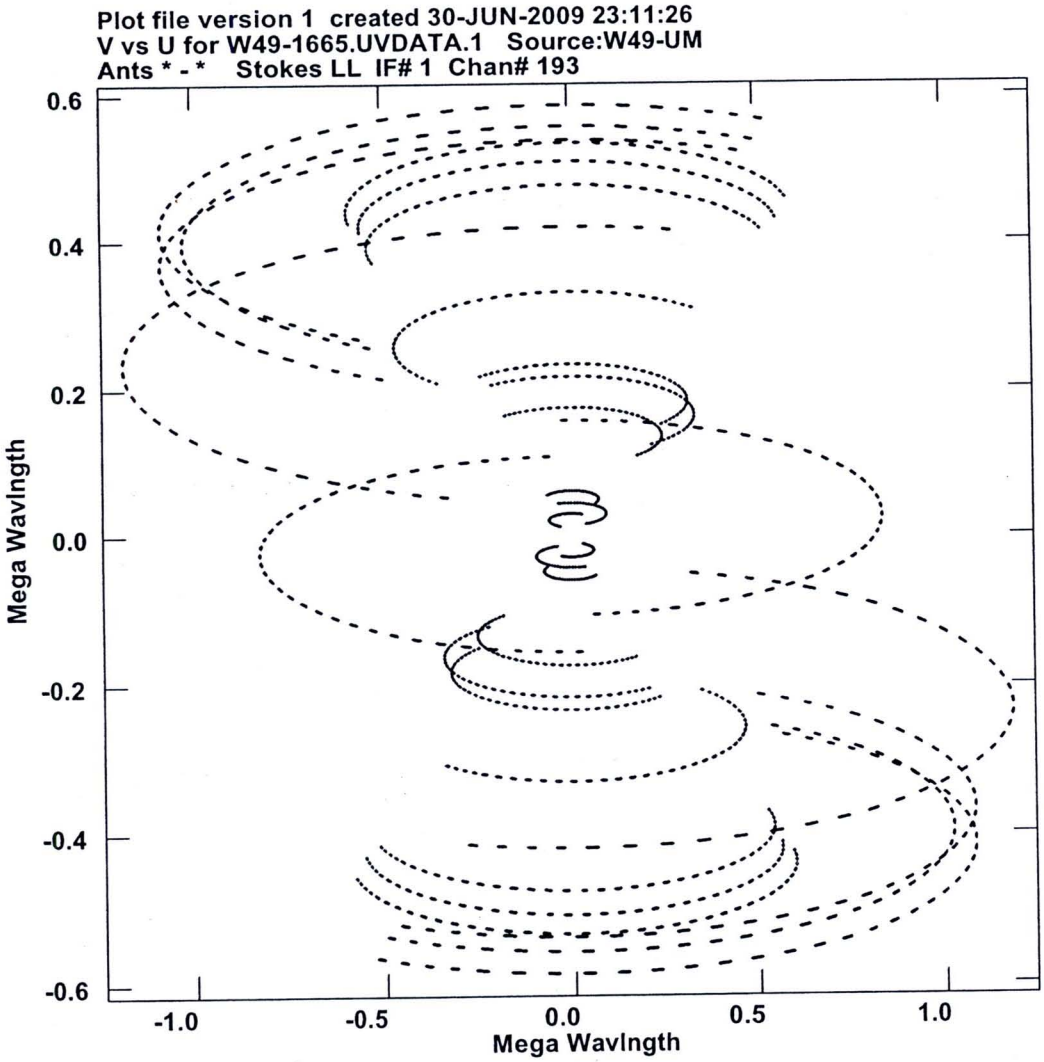

Figure 3.4 The u - v coverage at 1665 MHz for the source W49 A.

3.3.2 OH and CH_3OH Masers at 5 cm

Observations were made of S140-IRS1 and W49 A on 2008 February 15 and 2006 February 12-13 respectively at the frequencies of the 6 GHz excited state OH masers using all the MERLIN telescopes except the Lovell (Mk2, Darnhall, Tabley, Knockin and Cambridge). Observations were made of two maser transitions: the 6030.747MHz (F=2-2 hyperfine transition of the $^2\prod_{3/2}$, J=5/2 excited-state OH): 6035.092 MHz (F=3-3 hyperfine transition of the $^2\prod_{3/2}$, J=5/2 excited-state OH). Observations were made only of W49 A at the methanol maser frequency - during the period 2006 February 12-13. This observation, which also used all the telescopes except the Lovell, was of the 6668.518 MHz ($5_1 \rightarrow 6_0$ transition of A^+ methanol class II) spectral line. The longest baseline was 217 km, giving a synthesized beam size of 47 mas at 6.0 GHz. Spectral line data were taken using a 0.5-MHz bandwidth, centred at a line frequency corrected to the same Vlsr, as the ground state 1.6 GHz observations. The band was sub-divided into 512 frequency channels, giving a velocity span and resolution of 24.9 km s^{-1} in 0.049 km s^{-1} channels at 6.0 GHz and 22.5 km s^{-1} in 0.044 km s^{-1} channels at 6.7 GHz. Table 3.2 lists the detail of the methanol observations of W49 A.

3.3.3 H_2O Masers at 22 GHz

The observations of the $6_{16}-5_{23}$ H_2O transition (rest frequency 22.235079 GHz) were only made in the two parallel hands of circular polarization (LL-RR). The two hands of polarization were calibrated separately, but all the images were made in total intensity since no Zeeman splitting at the frequency resolution used was expected. 3C273 was used to set the flux scale based on monitoring data kindly provided by H. Teresranta (Metsahovi). 3C273 was also observed for a full track on 1998 January 24 in order to obtain a model for the flux and baseline calibration, since it was slightly resolved at this epoch. However, it appeared to be point-like in 2004 at MERLIN's resolution. Further details of MERLIN 22-GHz spectral-line data processing techniques have been given in Richards et al. (1999).

3.3.4 5-GHz continuum

Hoare (2006) observed the 5-GHz continuum emission from Sl40-IRS1 with MERLIN in 2000. These data were retrieved from the archive and re-imaged using a 2500-Mλ taper to give a restoring beam of 132 × 122 milli-arcsec. A shift in the source position was also made to take account of a more recent and better position for the phase-reference source RA $22^h19^m\ 18\overset{s}{.}22$ and Dec. 63° 18′ 46″.78.

3.4 Data Reduction

In section 3.1, it was very briefly shown that the on-line processed data output from MERLIN represents values for the Fourier Transform of the Sky Brightness Distribution, from which the structure of a source, if within the observation beam and of limited size, can be determined. However, these data have been corrupted

by changes in the source emission from the source as it passes through the Earth's atmosphere and the receiver system. Each modifies the data, with the result that the observed visibilities often show little resemblance to the original emission. The calibration process involves determining and applying corrections to recover the original coherence function, so that the imaging procedure can give a better representation of the sky brightness.

3.4.1 Initial Calibration

The initial processing of the MERLIN data was carried out using 'local' software called the `d-program`, the output from which in FITS format was further processed using the standard package, AIPS. The d-programs were used for initial data editing, preliminary calibration of the telescope flux scales, bandpasses, complex gains and also the application of gain-elevation corrections. The output FITS files were read into the AIPS package, which was used to continue the reduction process until final maps of the target source from the data were obtained.

In order to make good quality maps, the quality of the raw data is important. Bad data must be removed or edited out. This is done using the programme, `dplot`, which can be used to plot the raw amplitudes and phases against time, and to delete data that is bad or perhaps viewed as being suspect. The visibility amplitudes or phases of the raw data can also be plotted as a function of channel using the program `splot`. This is useful in deciding the bandwidth needed when initially planning spectral line observations, and also to identify the signal in spectral-line data if the **target** is strong enough.

3.4.2 Initial Data Processing and Editing Data in d-program

To make the explanation of the calibration and data reduction processes as clear as possible, we use the example processes of S140-IRS1 at 1665 MHz for explanation. The results of S140-IRS1 are presented in Chapter 4. The data for S140-IRS1 were listed using `dlist` which gives details of the frequencies, telescopes, polarizations and number of channels for each scan. The calibrators used in this case are flux amplitude calibrator **point-cal; 3C84**, phase calibrator **ph-cal; 2221+625** and polarization position angle calibrator **pa-cal;3C286**. Interactive editing was performed using computer mouse cursor. The task `dplot` allows various calibration to be applied. The selected baseline are plotted with amplitude in red and phase in green for one polarization and all channels. The task `dplot` is used to delete isolated amplitudes which too high or too low and where a particular telescope has very low amplitude and noisy or random phase. Data can be edited by deleting time-ranges, clipping discrepant amplitudes or zapping individual points. Editing was done for all baselines of the specified source. For a given baseline, editing is applied to all channels and polarizations. The editing in `dplot` was performed on **3C84** and **3C286**. The larger amounts of S140-IRS1 and **2221+625** data were edited in AIPS because there are problems using d-program in editing the large data set. The program `dplot` was also used to derive the flux of the primary calibrator source. The flux density of **3C84** can be found from the ratio of raw amplitudes on **3C84** to those on **3C286** multiplied by the

flux of **3C286** which is already known (for example, 13.642 Jy at 1662.800 MHz, this value is calculated from the VLA formula with 1999.2 coefficients). **3C286** is a well-known non-variable source but is resolved by MERLIN at 1.6 GHz on the longer baselines. **3C84** is a point source at that frequency but it is variable. The `dplot` was used to apply gain elevation correction and determine the raw amplitudes of **3C286** and **3C84** on the short baselines. The flux primary of **3C84** are ~20 Jy (1.6 GHz) and ~15 Jy (6.0 GHz). The program `tdproc`[3] is used to write a calibration file and then apply the corrections to the data and write them out in FITS format. The command `<dcal>` averages the selected time-range of data and automatically selects an antenna near the centre of the array to define the phase of its data in the reference channel as the origin. All data is then converted to the FITS format using the command `<dfits2000>` for transferring data to process in AIPS.

3.4.3 Initial Data Processing and Editing Data in AIPS

After being loaded into AIPS, the FITS files which had the same configuration were combined into a single multi-source file. In the case of S140-IRS1 and W49 A, three multi-source files had to be created. The first one contained the data on the target source, the second one contained the amplitude calibrator source and polarization position angle source on narrow band data (NB), and the last one contained the data on the phase calibrator source, the amplitude calibration source together with the polarization position angle calibrator source on wideband data (WB). The visibilities in these multi-source files were sorted in increasing time and baseline order.

This is the description for S140-IRS1 data at 1665 MHz. For other frequencies, the same processes are also used. Data from the FITS files were loaded into AIPS catalog file by the task `FITLD`. Three files are loaded as the following filename.

1. S140-1665NC.FITS - This is the file for the point source **3C84** and polarization position angle source **3C286** which were observed in NB.

2. S140-1.6WC.FITS - This is the file for the phase calibrator source **2221+625**, point source **3C84** and polarization position angle source **3C286** which were observed in WB.

3. S140-1665.FITS - This is the file for the target source S140-IRS1 which was observed in NB.

All three files were loaded into AIPS and classed as .UVDATA with 3 extension tables;

1. HI - a history file

2. AN - an antenna table for array geometric data, date, frequency, polarization,etc.

[3]The upper limit FITS file is 2 GB.

3. FQ - a frequency table

The task INDXR writes an index file for the uv-database. It creates a new NX table and a new CL table with 0.5 minute intervals. In the case of S140-IRS1 at 1665 MHz was observed by using 7 telescopes including Lovell. The task UVFLG uses to delete specific the shortest baseline between Mk2 and Lovell due to confusing signal. The task SETJY is used to set flux density for all sources, and the task IBLED is used to edit all bad data from the remaining baseline. IBLED is an interactive editing task which displays specified data on the AIPS TV and uses the mouse and keyboard to delete bad data. The flag table (FG) is created and updated with flagging information.

3.5 Calibration

The processes described in the previous section created multi-sources files, each of which contains many calibrator sources and one file contains only target source. The visibility data are saved in time-baseline order. Calibration processes also create other tables attached to the data file, including

1. BP for bandpass calibration
2. CL specified 0.5 minute interval of calibration table
3. SN for gain solution from the calibration routines

The flowcharts of calibration process can be shown in Appendix A. The detail in each step is described in each section as follow.

3.5.1 Amplitude and Bandpass Calibration

The task SETJY was used to set the point source calibrator flux of **3C84** to 20 Jy. The LSR velocity in the central channel (256) is -8.00 km s^{-1}. The task SETJY enters source information into the SU table. The task CALIB was run on point source calibrator **3C84**. This task determines the calibration to be applied to uv-data of **3C84** given a model of the source. The SN table will be left for the multi-source input data file. Solutions are stored in the SN table. For multi-source data, previously not applied SN tables can be smoothed and applied to the specified CL table before determining the new calibration constants. The task CLCAL applies solutions from a set of SN tables to selected entries in one CL table and writes them into a new version of the CL table which will apply to calibrate the uv-data. The task BPASS is used to determines the calibration constant for making the whole bandwidth have equal signal response. This creates a bandpass table (BP) attached to the multi-source file. Checking the BP table in each baselines by using task POSSM and aparm(8)=2.

3.5.2 Phase Offset at Different Frequencies

In the case of the target source is observed in NB and phase calibrator is observed in WB. There will be a phase offset between the different observing

configurations. Therefore, after loading the data into AIPS, carry out the bandpass calibration as mentioned above for NB. Copy the SN table of **3C84** WB contains the phase corrections across to S140-1665NC.UVDATA, this will create a new SN version (for example, SNX). Use SNPLT to plot and compare the phase range between SNX and SNY (phase correction for **3C84** NB). Check the time labels by using task TABED. After that use CLCAL to interpolate between the CL1+SNX, producing CLY+1. To find the phase offset, use CALIB for phase-self-calibration of the **3C84** at the NB, applying the last CLY+1, producing the newest SN table (SNX+1) and copy this table to target source.

3.5.3 Mapping Phase Calibrator

To make a map of the phase calibrator **2221+625**, first of all use the task CALIB is run using **2221+625** data and using reference telescope 4 to do self-calibration. In the first cycle of self-calibration, run the task CALIB by using point source model with the parameters refant 4, calsour '2221+625', solint =1, aparm(1)=3, aparm(7) =3 and solmode 'P'. After running, CALIB task generates SN table. Interpolation solution table to CL table using 2PT. Making a map by using the task IMAGR and use parameters docalib=1 and appropriate gainuse. In the second cycle, use image from the first cycle and positive clean components before the first negative to calibrate uv-data and decrease the solution interval. Then interpolate solution table into CL table. Self phase and amplitude calibration is repeated and solution interval is reduced until the satisfy map is produced. Editing data is done again to delete bad data which could not properly calibrated. Re-map it again and compare the result map with the previous version. Two SN tables contain phase and phase & amplitude from the last **2221+625** maps are copied to file target source S140-1665.UVDATA by using the task TACOP.

3.5.4 Polarization Calibration

Task PCAL[4] is used to correct for polarization leakage. It will only work on single-channel data in multi-source format. To be safe many calibration tables in S140-1.6WC.UVDATA by using task TASAV before splitting data. The point source calibrator **3C84** was split out to a single source file by the task SPLIT and run MULTI for creating the multi-source format. Task SETJY is used for setting the flux density in the new SU table. After used the task PCAL, copy AN table by using task TACOP to S140-1.6WC.UVDATA.

The task CALIB is run by assuming a point source on the polarization position angle **3C286** and interpolating the solution to the CL table. After that the L-R phaser is found by make clean maps in Stokes I,Q and U by using the task IMAGR. Combine Q and U maps by the task COMB and used opcode 'poli' and 'pola'. In the opcode 'poli' each pair of pixel in Q and U maps are combined by equation;

$$\mathrm{PPOL} = \sqrt{\mathrm{Q}^2 + \mathrm{U}^2} \tag{3.1}$$

[4]Due to the peak flux of OH masers at 6 GHz is weak therefore this task is not necessary to do if we could not find any spectrum of target source.

$$\text{PANG} = 0.5 \times \arctan\frac{U}{Q} \tag{3.2}$$

From the combined maps, run IMSTAT on 'poli' maps and IMVAL on 'pola' map. The angle value was the Polarization Angle (PA) then the polarization angle calibrator **3C286** will correct should equal to 33-PA degrees. Another easy method can check the PA is task LISTR. This task used to find the the apparent PA and report values for the phase of the cross-hands of polarization for each baseline followed by the average, equivalent to 2PA then the correct angle value should be 66-2PA degrees. The task CLCOR is used to correct the polarization angle of MERLIN data and used opcode 'polr' on Stokes 'L' if the AN table does not already contain corrections derived. This opcode is used only once because it modifies both the CL table and the AN table. This modified CL table is used to make a map of the polarization calibrator **3C286**. I-map, poli-map and pola-map are used to make the polarization map of **3C286** by the task PCNTR.

3.6 Mapping of Target Source

Before making the map of S140-IRS1, we have done the amplitude calibration and bandpass calibration on file S140-1665NC.UVDATA which is composed of sources **3C84** and **3C286** in 512 channels but the phase calibrator is on file S140-1.6WC.UVDATA. We repeat the process of polarization correction on S140-1665NC.UVDATA, because our source and the phase calibrator were observed in different frequencies and different bandwidths, so we can not concatenate them in to the same multi-files. Hence We must do the same basic processes for them on a separate files. After finished the calibration process, copy many tables of calibration across to target source file S140-1665.UVDATA. After that the AN table which is solved for polarization residual and the SN table are copied fromthe S140-1.6WC.UVDATA file to the S140-1665.UVDATA file. The task CLCOR is run using opcode 'phas' to rotate phase in CL table through the specified value inclcorparm(1). The solution in SN table is interpolated to CL table. This solution must have the same date and time as same as CL table. In the case of difference in date and time we must correct it by using TABED before we interpolate solution in SN table to CL table. After applied every tables to target source, we can check the brightest channel from Stoke LL and RR by using task POSSM. In the case of the spot of maser is shifted far away from the field centre, try to do the big image by arranging the size of image until you can see the spot. There are two methods for mapping the target source as follow;

1. In the case of methanol maser which is observed at 6.7 GHz in the star-forming region W49 A, we select a channel which all features in RR and LL maps have the same position as a model for self-calibration. It would be the best if the selected channel has only one feature. Using that channel as a model for self-calibration in Stokes I. Self-calibrations are carried out by

using the same method as we have done for self-calibrations of the phase-calibrator. After the last best map for that channel is carried out, its last CL table is used for mapping all of the remaining channels.

2. Comparing the spectra of Stokes LL and RR and select the strongest peak flux only from one Stokes for example Stoke LL is stronger than Stokes RR then used Stokes LL as the first calibration. It would be the best if the selected channel has only one feature and the same position for both Stokes. Using that channel as a model for self calibration in Stokes LL. Self-calibration is carried out by using phase solution only and used task SNCOR which has opcod 'pcop', sncorprm(1)=2 will copy the polarization solution across from Stokes LL to Stokes RR. Applying solution by task CLCAL and then repeat this process until get the last best map for Stokes LL. The finalized self-calibration for Stokes LL used phase & amplitude solution. After that self-calibrations by using the strongest channel of Stokes RR as the model. Repeating the method as Stokes LL excepted that the task SNCOR should used opcode 'zphs' for forcing phase of Stokes LL to be zero. After the last best map for that channel is carried out then the finalized self-calibration for Stoke RR used phase & amplitude solution. Normalized the strongest flux from Stokes L by using the task SNCOR opcod 'norm' and opcod 'zphs', its last CL table is used for mapping all of the remaining channels.

3.6.1 LL,RR,I,Q,U,V Maps

Before making all channel maps, the uv-data was re-weighted by the task WTMOD. The sensitivity gain weighting for telescopes are given in the Table 3.3. Mapping of all 512 channels for LL, RR and each Stokes parameter (I,Q,U,V) was carried out by the task IMAGR. The maps were used with a cell size 0.045 $\times$ 0.045 arc-second and 0.005 $\times$ 0.005 arc-second at 1.6 GHz and 6.0 GHz respectively. It will be usefulness if the map size is 512 $\times$ 512 pixels. The contour maps were generated by the task KNTR at different noise levels and printed out by the task LWPLA.

3.6.2 Polarization Maps

Polarization maps of the target sources were made using the same processes used to make the polarization map of the phase calibrator. The combination of Q and U maps were combined using the task COMB with opcode 'poli' and 'pola' for polarization intensity and polarization angle maps respectively. Each feature was mapped in polarization showing the field strength and direction (derive from 'poli' and 'pola' maps) superimposed on the I map contours.

3.7 Map Analysis

After we get the best maps of all spectral channels and polarization, the next process is the analysis of these maps to extract the physical information. The analytical processes which were carried out are described below.

3.7.1 Identification of the Maser Features

The channel maps of S140-IRS1 and W49 A[5] were searched for maser spots. Care was taken to avoid artifacts due to noise or beam side-lobes. Peaks of over $3\sigma_{\text{noise}}$ occurring in three successive channels were identified as spots, making up a maser component. A two dimensional Gaussian component was fitted to each patch of maser emission in each spectral channel using the task `JMFIT`. This task is usefulness for the maps contain a few components. The components which coincided with the side lobes of the MERLIN beam were rejected. This was done for Stokes LL, RR and I, the results show the position and intensity of each maser component. In the case of images contain multiple components of a similar size to the beam (as shown in Figure 3.5). This can be done automatically using `SAD` routine[6],with a cut-off of $3\sigma_{\text{noise}}$, and we rejected any components coinciding with sidelobes in the dynamic-range limited channels. After run the task SAD, it will generate MF table in each channel. There is a local AIPS task `MFQUV`[7] which measures the polarized flux density at the position of components in an MF table. Before starting AIPS, use the command `setenv WORK /scratch/hecate_1/amsr/AIPSTASKS/PJD/` and type `VERS 'PJD'` inside AIPS. The task `MFQUV` uses Stokes I, Q, U and V data-cubes as the four input files. The results will be inserted to the MF table of Stokes I and we can select some columns for analyzing data by using task `PRTAB`. In order to collect the Gaussian fits output by `SAD`, a `FORTAN` language called `HAPPY` was developed. `HAPPY`[8] takes the strongest emission Gaussian fit in the given channel map and looks in the nearest channel map above for the nearest Gaussian spatially separation. The results show the physical information in each feature as the text and numerical files which are usefulness for analyzing the physical properties further.

3.7.2 Measuring Maser Positions and Intensities

Consider the celestial sphere which represents the positions of masers in each time just like in Figure 3.6. The position angle in the sky towards that is the angle ψ between the direction on the celestial sphere, and the northward direction as shown in Figure 3.6. If we consider the eastward direction as well on this sphere (at right angles to the northward direction); we can break up the maser motion into its northward component $\mu cos\psi$, which is just its maser motion in declination, μ''_δ, and into its eastward component, $\mu sin\psi$, which, however, is not equal to the maser position, μ_α, in R.A.

The reason for this is that the maser position in R.A. is measured along the equator, which is a great circle, whereas the eastward displacement, $\mu sin\psi$, is measured along a small circle. In Figure 3.6, which shows the annual displacement

[5]This source is very complex and extended therefore we created a short script used runfil into AIPS for searching many fields centre covered 275×275 arcsec in RA and Dec offset respectively. The script is described and shown in Appendix B, Section B.1

[6]The script is described and shown in Appendix B, Section B.2

[7]This task can be operated only from LINUX machine rather than SUN system.

[8]This software was developed by Dr.Mark Wright and Dr.Malcolm D. Gray.

of a maser on the celestial sphere, we see that $\mu'' sin\psi$ is just equal to $\mu_\alpha cos\delta$. Then the position of masers in right ascension are $cos\delta$ when δ is declination.

From Hutawarakorn (1997), maser emission was seen in the channel maps in discrete spots. The position and intensity of each spot was measured by fitting two dimensional Gaussian components using a least squares technique (the AIPS task JMFIT). The individual components were resolved and usually only one but sometimes up to three were found per channel. The appropriate number of multiple Gaussion components were fitted where they appeared to be blended.

The positional uncertainty of each component is given by half the beam - width in R.A. or Dec. divided by the signal to noise ratio for that component (Condon, 1997). Series of components were found in 3 to 15 succesive channels in the same position to within the uncertianty and these were assigned to maser features. Components were rejected unless they were above $3\sigma_{noise}$ in at least three successive channels.

The positions and velocities of features quoted in the results table (in Chapter 4) are the flux weighted means of the positions and velocities measured in individual channels;

$$X = \frac{\sum_i X_i S_i^2}{\sum_i S_i^2}, \tag{3.3}$$

where
X is the mean R.A., Dec. or velocity of a whole feature;
X_i is the R.A., Dec. or velocity of an individual component allocated to that feature;
S_i is the peak flux of an individual component allocated to that feature;
and $\sum_i$ is the sum over the channels containing that feature.

The standard deviation of the sum of all component positions within a feature gives the feature positional uncertainty. The peak flux density given in the result tables is measured from the brigthest component in each feature.

3.7.3 Proper Motion

The proper motion of a star is its angular change in position with time as seen from the Sun. It is measured in seconds of arc per year (arcsec/yr). This contrasts with radial velocity, which is the time rate of change towards or away from the viewer, usually measured by the Doppler shift of received radiation. The proper motion is not entirely "proper" (i.e. intrinsic to the star) because it includes a component arising from the motion of the Sun itself. The proper motion is defined by two quantities: its magnitude and also the direction or position angle of the motion itself (as shown in Figure 3.7). The first quantity is measured in seconds of arc per year, and the position angle of the motion is relative to directions on the celestial sphere such that 0 degrees is to the North and 90 degrees is to the East.

3.7.4 Position Accuracy

The accuracy of the absolute masers position measured in this thesis is limited by four factors: (1) the position accuracy of the phase calibrator: (2) the accuracy of the telescope positions: (3) the relative position error depending on the beamsize and signal-to-noise ratio; and finally (4) the atmospheric variability that plays an important role especially at 22 GHz depending on the angular separation between the phase-calibrator (for example **2221+625**) and the target source. The first two factors are frequency independent and were estimated to be 5 mas (given by the MERLIN calibrator catalogue) and 10 mas respectively (Daimond et al., 2003). The other two factors are frequency dependent. The relative position error, given approximately by the beam size/signal-to-noise ratio, leads to uncertainties in the position of 17 and 4 mas at OH and H_2O maser lines respectively. Factor (4) is inferred from the quantity of the phase of the calibrator separates from target source. With a separation of 5°, we can estimate this error is 20 mas. All these errors add quadratically to give 30 mas at 1.6 and 22 GHz and 15 mas at 5-6 GHz, as the total systematic error in the absolute positions measured and used as comparing our results with other publications.

3.7.5 Polarization Determination

After fitting Gaussian components to the LCP and RCP spots, the Zeeman pairs and linearly polarized features were identified. The spots in the Stokes parameters I maps were fitted to obtain the value of Stokes parameters Q, U, and V were measured by using the AIPS verb IMVAL at the pixel of Stokes I peak.

The rms noise σ_I, σ_Q, σ_U,σ_V, and σ_P were directly measured from off-source region of the channel maps. The parameters of linear polarization(m_L), circular polarization(m_C) and total polarization(m_T) were determined from the following equations;

$$m_L(\%) = \frac{P}{I} \times 100, \tag{3.4}$$

$$m_C(\%) = \frac{V}{I} \times 100, \tag{3.5}$$

$$m_T(\%) = \sqrt{m_L^2 + m_C^2} \times 100. \tag{3.6}$$

The percentage of the linear and circular polarization values were set to zero in the case of $P < \sigma_P$ and $V < \sigma_V$, respectively.

Uncertainties in percentage of linear and circular polarization non-zero m_L and m_C are

$$\sigma_{m_L} = m_L \sqrt{\frac{\sigma_P^2}{P^2} + \frac{\sigma_I^2}{I^2}}, \tag{3.7}$$

and

$$\sigma_{m_C} = m_C \sqrt{\frac{\sigma_V^2}{V^2} + \frac{\sigma_I^2}{I^2}}. \tag{3.8}$$

The uncertainty of the percentage of total polarization can be estimated from

$$\sigma_{m_T} \simeq \sqrt{\sigma_{m_L}^2 + \sigma_{m_C}^2}. \tag{3.9}$$

For a component with non-zero fractional linear polarization position angle uncertainty σ_X can be estimated using

$$\sigma_X \simeq 0.5 \times \frac{\sigma_P}{P}. \tag{3.10}$$

The position angle uncertainties quoted in the result tables do not include the error from removing the instrumental polarization. This error is estimated to be $\leq 1°$.

3.7.6 Zeeman Pair and Magnetic Field Determination

The magnetic field in the compact maser sources could be measured from the effect of Zeeman splitting in their LHC and RHC spectrum. The Zeeman pairs are identified as maser features which appear on the maps of the opposite circular polarizations at the same position. The maser features in both LHC and RHC maps are considered to appear in the same position if they coincide within the positional uncertainty. In the case of maser features appearing in clumps on both maps, the criteria for the position coincidence must be carefully investigated to remove the effect of the clumpiness. When a pair of maser features of opposite polarization coincides it is considered to be Zeeman pair. The velocity difference is measured from their spectra. The magnetic field intensity is then calculated from Chapter 2 Table 2.2, which is a part of table given by Davies (1974).

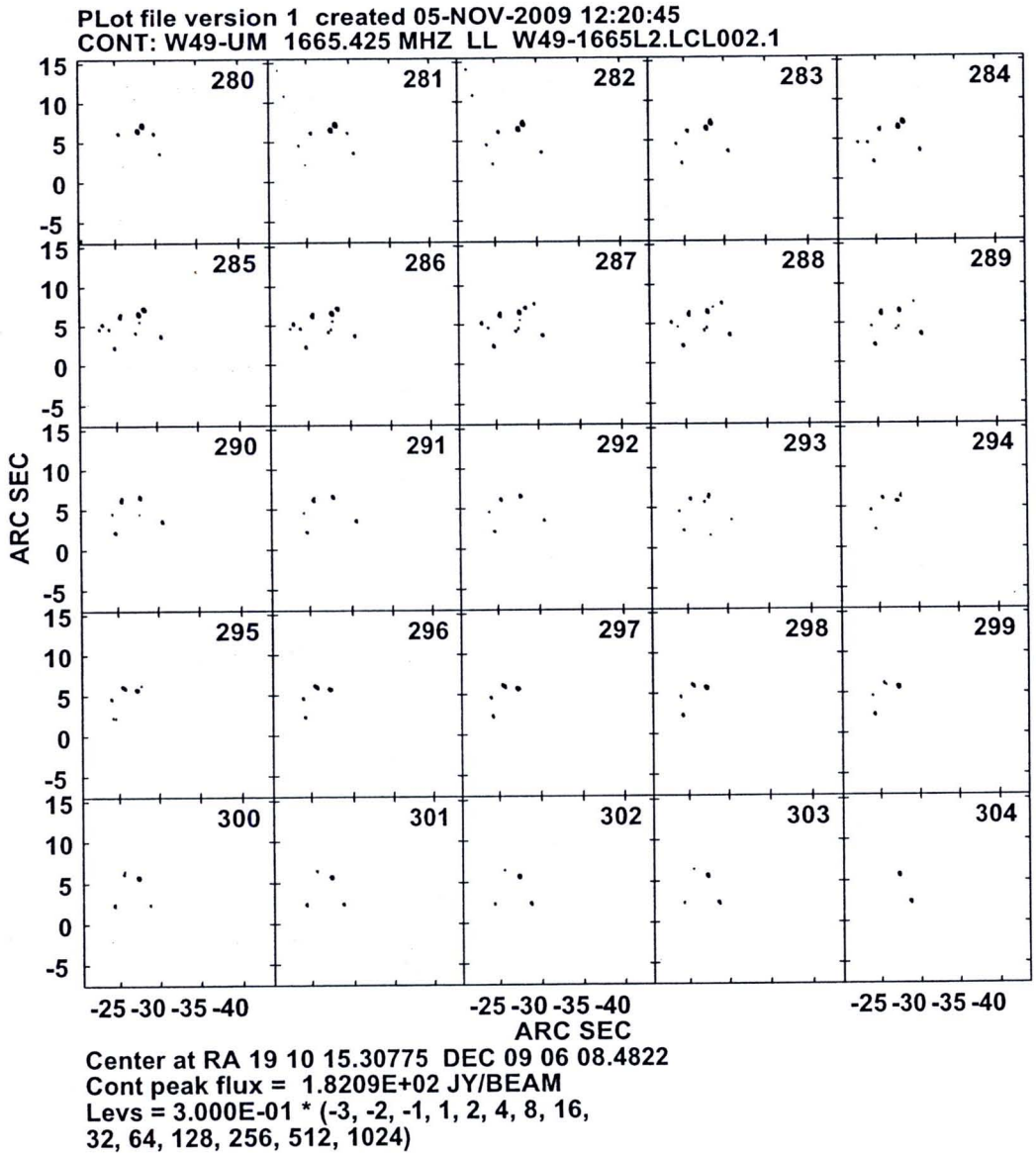

Figure 3.5 Map of Stoke LL by using command `KNTR` from channel 280 to 304 which contains many components in the W49 A at 1665 MHz.

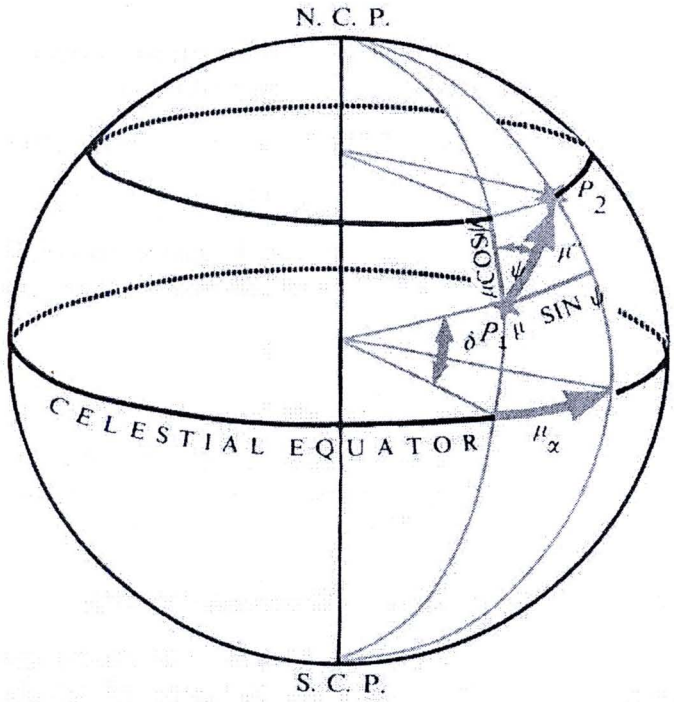

Figure 3.6 The position of maser in declination and right ascension (Motz and Duveen, 1977).

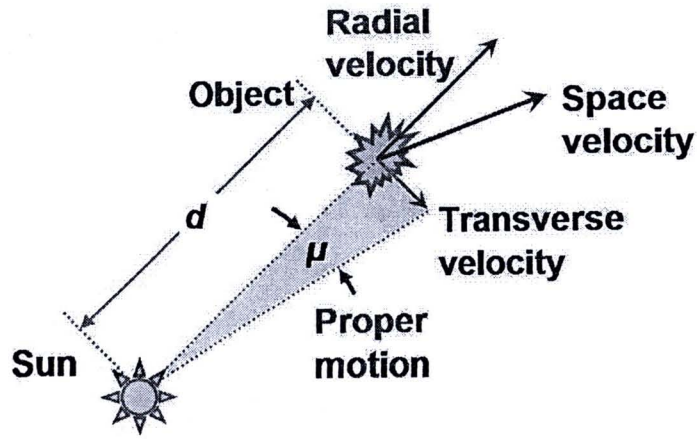

Figure 3.7 Relation between proper motion and velocity components of an object. The object is at a distance, d, from the Sun, and moves at an angular rate of μ radians/s.